Modification of $BaYMn_2O_{5+\delta}$ perovskite in an aspect of development of oxygen storage technology in perovskite oxides

Alicja KLIMKOWICZ, Kun ZHENG, Grzegorz FIOŁKA, Konrad ŚWIERCZEK – AGH University of Science and Technology, Faculty of Energy and Fuels, Department of Hydrogen Energy, al. A. Mickiewicza 30, 30-059 Krakow, Poland

Please cite as: CHEMIK 2013, **67**, 12, 1199–1206

Introduction

Storage of gases in solids is commonly associated with hydrogen storage. It can be realized as an absorption-type storage in a form of various hydrides, and adsorption-type storage in carbonaceous materials and zeolites. Such types of H_2 storage seem to be an alternative to high-pressure or cryogenic tanks, due to a possibly of higher hydrogen storage density [1]. Oxygen storage is rather understood as a usual, high-pressure storage of O_2 in various tanks, which are used in industry, chemical and physical laboratories and in hospitals. However, starting from 1980s, so called oxygen storage materials (OSM) are being used in automotive industry, where they serve as a reservoir of oxygen, needed for an efficient work of three-way (oxidation-reduction) catalytic converters [2]. The main reactions, taking place in these converters are: reduction of nitrogen oxides to nitrogen and oxygen, oxidation of carbon monoxide to carbon dioxide, and oxidation of unburned hydrocarbons to CO_2 and water. All of these reactions are effectively catalyzed when the air to fuel ratio is near stoichiometric one, which requires usage of computerized, closed-loop feedback fuel injection systems, equipped with one or more oxygen sensors. Typically, precious metal-based catalysts are used both, in reduction and oxidation zones. Under rich conditions (excess of fuel), occurring for instance in the case of rapid acceleration of the vehicle, not enough oxygen is available in the exhaust gases stream for the oxidation reactions. At this point, the needed oxygen is released from OSM material, which therefore can be described as the auxiliary catalyst. Oxygen storage capacity of OSM is therefore one of the main indicators of quality of such catalyst. Under lean conditions (excess of air), depleted OSM will absorb oxygen back, and will help to catalyze decomposition of NO_x [2].

Currently commercialized OSMs are mixed oxides from ceria-zirconia (CZ) or ceria-lanthana (CL) system, with newer generations having Al_2O_3 additions. In the case of $Ce_{0.5}Zr_{0.5}O_2$ material, reversible oxygen storage capacity significantly exceeding 500 μmol of O_2 per gram of the compound can be obtained [3].

The physicochemical basis for the reversible oxygen storage is related to the following reaction:

$$Ce^{4+}_{1-x}Zr^{4+}_{x}O_2 = Ce^{4+}_{1-x-y}Ce^{3+}_{y}Zr^{4+}_{x}O_{2-y/2} + y/4O_2 \quad (1)$$

At low oxygen partial pressures (excess of fuel), the above reaction is shifted to the right, in oxidizing atmospheres (excess of air), it is shifted to the left. This reaction utilizes ability of cerium to reversible changes of its oxidation state in fluorite-type structure (Ce^{4+}-Ce^{3+}), as well as mobility of oxygen ions. The reversible oxygen storage capacity can be also expressed in terms of weight change, and for the mentioned $Ce_{0.5}Zr_{0.5}O_2$ material the maximum capacity calculated according to the Eq. 1 is equal to about 2.8% weight.

Apart from the transportation industry, OSM materials exhibiting high capacity may find their usage in many important and developing technologies and industrial processes, as well as in applications where precise control and possibility of fast changes of the oxygen partial pressure in gas atmosphere are required. Among them: air separation, solar water splitting, non-aerobic oxidation, high-temperature production that require high-purity oxygen, oxy-fuel and chemical looping combustion for so called clean coal energy production, production of synthesis gas, inert gas purification, and Solid Oxide Fuel Cell technology seem to be possible application areas.

Currently there is an ongoing research devoted to improvement of OSMs, especially in an aspect of higher reversible oxygen capacity and faster reduction/oxidation kinetics. New materials are being proposed, and among them Pr_2O_2S-$Pr_2O_2SO_4$ system should be mentioned, as the one with the highest capacity of the order of 9.3 %weight. Unfortunately, irreversible sulfur evaporation strongly limits its application [4]. Alternatively, $BaYMn_2O_5$-$BaYMn_2O_6$ system was proposed, which in addition to a high reversible capacity possesses also the highest oxygen intake rate, estimated to be 25% weight·min^{-1} at 500°C [5]. These materials belong to A-site ordered family of perovskite-type oxides, which structure can be derived from simple ABO_3-type perovskites.

Basic structure of ABO_3 perovskite oxides is cubic, with Pm-3m space group. It can be described as 3D network of corner-sharing BO_6 octahedra, in which A cations occupy all available 12-fold coordinated positions. Alternatively, it can be described as a dense, close cubic packing (ccp) type of network of AO_3, in which ¼ of octahedral sites is occupied by B cations. This structure is a base for many related, lower-symmetry structures, in which octahedral tilting, distortions, nonstoichiometry and ordering in A, B or oxygen sublattices may occur. Ordering of cations in perovskite structure often occurs due to a large difference of ionic radii and/or oxidation states between cations present at the same time either at A or at B site. While 1:1 rock-salt-type ordering is a rather typical one in $A_2BB'O_6$ materials, for $AA'B_2O_6$ oxides, layered ordering is the most common one [6]. Such ordering occurs also in the mentioned $BaYMn_2O_6$ material. Interestingly, it was found that during reduction, oxygen is preferentially removed from positions in yttrium plane, and all these positions are empty in $BaYMn_2O_5$. The change of δ between the fully reduced and fully oxidized material equals one mole per unit formula of $BaYMn_2O_{5+\delta}$. This in turn gives a very high, theoretical change related to the oxygen storage, equal 3.85% weight, significantly exceeding capacity of currently commercialized OSM materials. The published data indicate full oxidation of $BaYMn_2O_5$ taking place below 400 °C in oxygen and reduction of $BaYMn_2O_6$ occurring below 500°C in 5% H_2 in Ar mixture [5].

The presented paper shows possibility of modification of $BaYMn_2O_{5+\delta}$ in the aspect of development of oxygen storage technology, which is realized by chemical substitution of yttrium by gadolinium. $BaY_{1-x}Gd_xMn_2O_{5+\delta}$ (x = 0, 0.25, 0.5, 0.75 and 1.0) materials were studied in terms of their crystal structure and oxygen storage-related properties.

Experimental

Y-site substituted oxides with chemical formula $BaY_{1-x}Gd_xMn_2O_{5+\delta}$ (x = 0, 0.25, 0.5, 0.75 and 1.0) were synthesized

by a soft chemistry method. Respective nitrates were dissolved in deionized water in stoichiometric proportions. Ammonia salt of ethylenediaminetetraacetic acid (EDTA) was added as a complexing agent. The solutions were heated in quartz evaporators in air up to about 400°C. This resulted in the following processes: evaporation of water, sol-gel transition, decomposition of ammonium nitrite and EDTA, and finally, oxidation of residual carbon. The obtained precursors were thoroughly grinded in agate mortar and pressed into pellets. The actual synthesis was performed at 1100°C for 8 h, in atmosphere of 1 %vol. of H_2 in Ar, with flow of the gas of about 100 cm^3min^{-1}. Structural studies of the synthesized materials were carried out using Panalytical Empyrean diffractometer. Rietveld analysis of XRD data was performed using GSAS/EXPGUI set of software [7, 8], which allowed to provide detailed structural information about the samples. Thermogravimetric (TG) method was used in order to characterize oxygen storage properties of the obtained $BaY_{1-x}Gd_xMn_2O_{5+\delta}$ compounds. Measurements were done on powdered samples, obtained after grinding of sinters and sieving on 100 μm sieve. For reduction, 5 %vol. H_2 in Ar gas mixture was used, while oxidation process was studied in air. Gas flow of 100 cm^3min^{-1} and heating rate of 5 $deg \cdot min^{-1}$ were selected as experimental conditions. Isothermal reduction/oxidation was done at 500°C, it was carried out after 2th reduction of the considered material. All measurements were performed on TA Q5000IR apparatus.

Results and discussion

Structural and microstructural studies

Based on X-ray diffraction measurements with Rietveld analysis, it was possible to determine phase composition and crystal structure parameters (unit cell volume, unit cell parameters) of the synthesized materials. The results for reduced $BaY_{1-x}Gd_xMn_2O_5$ and oxidized $BaY_{1-x}Gd_xMn_2O_6$ (x = 0, 0.25, 0.5, 0.75 and 1) are shown in Table 1. All of the samples were identified as single phase, with no significant amount of secondary phases. For the reduced materials, P4/nmm space group, representing tetragonal crystal system was selected for XRD data refinement, based on the literature data for undoped $BaYMn_2O_5$ [9]. Rietveld analysis confirmed that all $BaY_{1-x}Gd_xMn_2O_5$ compounds possess such structure, with preserved layered arrangements of A sublattice i.e. gadolinium substitutes yttrium in one layer ($Y_{1-x}Gd_x$), while much bigger barium cations remain in the other layer. In the case of oxidized materials, such arrangement is also preserved, but the additional oxygen causes an appearance of a low symmetry distortion. Literature data for $BaYMn_2O_6$ does not give unequivocal answer about nature of this distortion [10, 11], however, precise neutron diffraction studies indicate very low symmetry, triclinic P-1 structure [12]. This structure was used for refinement of all oxidized materials. For samples with $x \leq 0.5$, such triclinic distortion seems to correctly describe the actual crystal symmetry. Figure 1 shows exemplary data for reduced $BaY_{0.5}Gd_{0.5}Mn_2O_5$ and oxidized $BaY_{0.5}Gd_{0.5}Mn_2O_6$ materials, with clearly visible distortion, appearing for the oxidized sample as a left shoulder of the most intense peak. Data for $BaY_{0.25}Gd_{0.75}Mn_2O_6$ shows minimal triclinic distortion, however, presence of higher symmetry structure cannot be excluded, due to very similar ***a*** and ***b*** unit cell parameters. Precise neutron diffraction studies, which are more sensitive for determination of fractional coordinates of oxygen anions, are necessary for clear description of this structure. Interestingly, oxidized $BaGdMn_2O_6$ exhibits the same tetragonal symmetry as the reduced material. Similar behavior was also observed for $BaSmMn_2O_5$-$BaSmMn_2O_6$ system [13]. The layered Ba-$Y_{1-x}Gd_x$ arrangement is presented in Figure 2, which shows visualization of crystal structure of reduced and oxidized materials. As can be seen, apart from ordering of A-site cations, the reduced materials also show charge ordering, as two distinctive positions for Mn^{3+} and Mn^{2+} are present in the structure [9]. Both of these positions are square pyramidal. For the oxidized materials, Mn^{4+} and Mn^{3+} cations should be present, due to a electroneutrality principle. However, much higher electrical conductivity of these samples indicates a significant delocalization of electrons near Fermi level, suggesting that charge ordering does not take place. For a clear description, this effect requires additional studies of transport properties of the considered materials. It is worth noting that all manganese cations are present in octahedral coordination in $BaY_{1-x}Gd_xMn_2O_6$.

Table 1

Structural parameters of perovskites from $BaY_{1-x}Gd_xMn_2O_{5+\delta}$ group

Composition	Space group	A [Å]	B [Å]	C [Å]	Volume V [Å^3]
Reduced materials					
$BaYMn_2O_5$*	P4/nmm	5.5496(1)		7.6548(1)	235.75(1)
$BaY_{0.75}Gd_{0.25}Mn_2O_5$	P4/nmm	5.5577(1)		7.6632(2)	236.70(2)
$BaY_{0.5}Gd_{0.5}Mn_2O_5$	P4/nmm	5.5642(1)		7.6711(1)	237.50(1)
$BaY_{0.25}Gd_{0.75}Mn_2O_5$	P4/nmm	5.5746(1)		7.6789(1)	238.63(1)
$BaGdMn_2O_5$	P4/nmm	5.5808(1)		7.6876(1)	239.43(1)
Oxidized materials					
$BaYMn_2O_6$*	P-1	5.5253(1) α = 90.01(1)	5.5198(1) β = 90.30(1)	7.6105(1) γ = 89.96(1)	232.11(1)
$BaY_{0.75}Gd_{0.25}Mn_2O_6$	P-1	5.5271(5) α = 90.00(2)	5.5240(5) β = 90.30(1)	7.6130(6) γ = 89.95(1)	232.43(4)
$BaY_{0.5}Gd_{0.5}Mn_2O_6$	P-1	5.5290(1) α = 90.01(1)	5.5273(1) β = 90.29(1)	7.6142(1) γ = 89.97(1)	232.69(1)
$BaY_{0.25}Gd_{0.75}Mn_2O_6$	P-1	5.5313(1) α = 90.01(1)	5.5314(1) β = 90.24(1)	7.6130(6) γ = 89.96(1)	232.86(1)
$BaGdMn_2O_6$	P4/nmm	5.5352(1)		7.6121(1)	233.23(1)

*Data from [13].

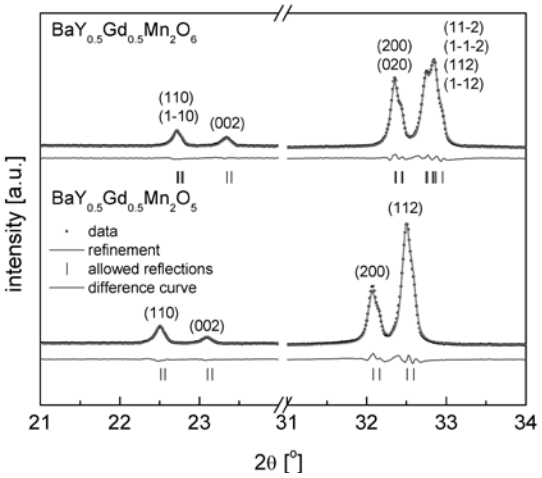

Fig. 1. X-ray diffractograms (selected range) with Rietveld analysis for $BaY_{0.5}Gd_{0.5}Mn_2O_5$ and $BaY_{0.5}Gd_{0.5}Mn_2O_6$

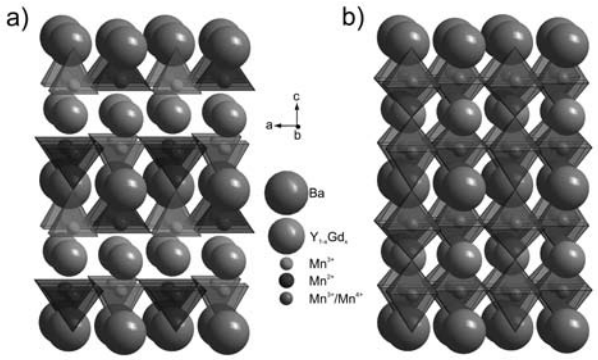

Fig. 2. Visualization of crystal structure of $BaY_{1-x}Gd_xMn_2O_5$ and $BaY_{1-x}Gd_xMn_2O_6$ Picture range corresponds to 2×2×2 unit cells

Exemplary SEM micrograph for $BaGdMn_2O_6$ compound is shown in Figure 3. The powder consists of sintered grains, which size is of the order of few micrometers. Similar microstructure was observed for all other materials, with no visible change between reduced and oxidized materials. Similarity of microstructure of the powders is very important, because it allows for a comparison of oxygen storage properties, shown below, as kinetics of the oxidation and reduction processes are strongly dependent on the specific surface of studied samples, as well as on grain morphology.

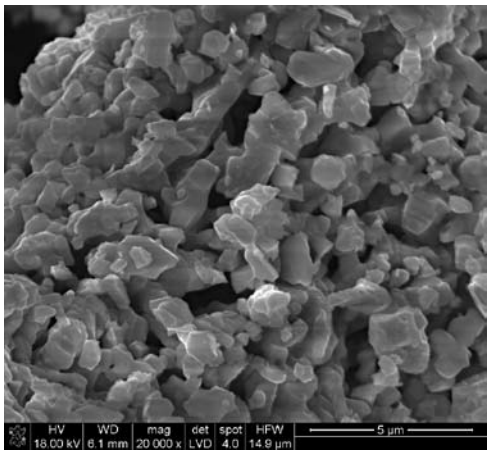

Fig. 3. Microstructure of $BaGdMn_2O_6$ powder as seen by SEM

Studies of oxygen storage-related properties

Results of thermogravimetric measurements are gathered in Figures 4÷6. Based on these data, all parameters related to the reversible oxygen storage process could be established for studied $BaY_{1-x}Gd_xMn_2O_{5+\delta}$. As can be seen in Figure 4, the reduced materials oxidize while heated in air. This process initiates above 150°C and for materials with higher Gd content occurs at lower temperatures. The recorded mass changes exceed 3% weight for all materials, which is significantly more, comparing to well known $Ce_{0.5}Zr_{0.5}O_2$, and are higher for samples with the increasing yttrium content. This effect can be understood taking into account changes of molar mass of the compound, when lighter Y^{3+} is substituted by heavier Gd^{3+} cations. Isothermal reduction kinetics, recorded at 500°C in 5 %vol. of H_2 in Ar, of previously oxidized $BaY_{1-x}Gd_xMn_2O_6$, are shown in Figure 5. For all the samples this process takes less than 20 minutes, however Gd-containing materials reduce much faster. Similar, isothermal oxidation kinetics in air is shown in Figure 6. One can see that for all studied materials this process is much faster, comparing to the reduction. This can be easily explained, as the oxidation was shown to be exothermic for $BaYMn_2O_{5+\delta}$ [14]. As the oxidation is much quicker, from the point of view of application, the reduction process needs to be optimized, and as shown in Figure 5, this effect was obtained by chemical substitution of yttrium by gadolinium. Summary of oxygen storage properties is given in Tables 2 and 3. One may notice that the measured, reversible capacity is almost equal to the theoretical one for all of studied samples. The calculated changes of oxygen content δ exceed 99% of the allowed changes between O5 and O6 composition (Tab.2). Furthermore, the fastest reduction rate and the lowest temperature of oxidation were recorded for $BaGdMn_2O_{5+\delta}$. This characteristic temperature of oxidation, defined as the one, at which 95% of the total mass change, occurs decreases from 375°C for $BaYMn_2O_{5+\delta}$ down to 305°C for $BaGdMn_2O_{5+\delta}$ (Tab. 3). Summarizing, an improvement of oxygen storage-related kinetics of reduction was observed for Gd-containing samples; however, it is accompanied by a decrease of the reversible capacity of the materials. These results are promising, as they indicate possibility of further improvements, which should be achieved by an appropriate selection of dopant cation.

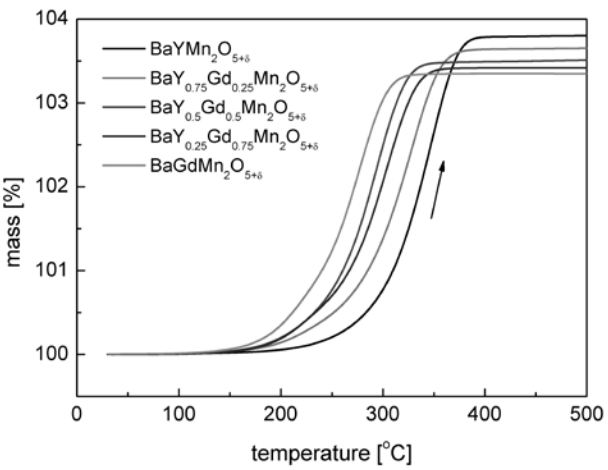

Fig. 4. Oxidation of $BaY_{1-x}Gd_xMn_2O_5$ in air

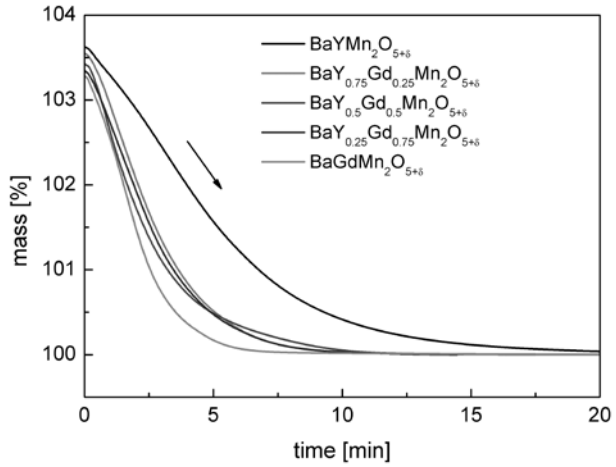

Fig. 5. Isothermal reduction at 500 °C of $BaY_{1-x}Gd_xMn_2O_6$ in 5 %vol. H_2 in Ar atmosphere

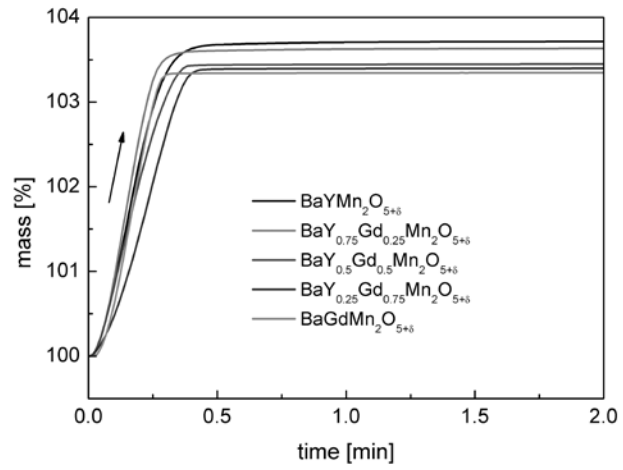

Fig. 6. Isothermal oxidation at 500 °C of $BaY_{1-x}Gd_xMn_2O_5$ in air

Table 2

Oxygen storage properties of $BaY_{1-x}Gd_xMn_2O_{5+\delta}$ (2nd cycle)

Composition	Theoretical capacity [% wt.]	Measured capacity [% wt.]	Change of the oxygen content δ [mol·mol^{-1}]
$BaYMn_2O_{5+\delta}$	3.85	3.63 3.82 in 5th cycle*	0.943 0.992 in 5th cycle*
$BaY_{0.75}Gd_{0.25}Mn_2O_{5+\delta}$	3.69	3.64	0.985
$BaY_{0.5}Gd_{0.5}Mn_2O_{5+\delta}$	3.55	3.45	0.972
$BaY_{0.25}Gd_{0.75}Mn_2O_{5+\delta}$	3.42	3.40	0.993
$BaGdMn_2O_{5+\delta}$	3.30	3.28	0.993

*Data from [13]

Table 3

Parameters of reduction and oxidation processes for $BaY_{1-x}Gd_xMn_2O_{5+\delta}$ (2nd cycle)

Composition	Characteristic temperature of oxidation [°C]	Rate of reduction at 500°C [min] (95 % change of total mass)	Rate of oxidation at 500°C [s] (95 % change of total mass)
$BaYMn_2O_{5+\delta}$	375	13.2	22
$BaY_{0.75}Gd_{0.25}Mn_2O_{5+\delta}$	360	6.9	18
$BaY_{0.5}Gd_{0.5}Mn_2O_{5+\delta}$	330	7.8	21
$BaY_{0.25}Gd_{0.75}Mn_2O_{5+\delta}$	335	7.0	23
$BaGdMn_2O_{5+\delta}$	305	5.0	16

Summary

$BaY_{1-x}Gd_xMn_2O_{5+\delta}$ (x = 0, 0.25, 0.5, 0.75 and 1.0) materials were successfully synthesized by a soft chemistry method. Introduced Gd^{3+} cations substitute Y^{3+} cations in their crystal positions, and for all reduced and oxidized materials, layered-type ordering in $BaY_{1-x}Gd_x$ is preserved. Oxidized materials exhibit triclinic distortion of crystal lattice, however, for $BaGdMn_2O_6$ tetragonal structure is present. The same tetragonal structure (P4/nmm symmetry) was confirmed for all of the reduced samples. Thermogravimetric measurements indicated reversible oxygen storage ability for all considered compounds. Materials containing gadolinium exhibit significantly improved reduction rate, which process is the essential one from the point of application. Additionally, Gd-containing $BaY_{1-x}Gd_xMn_2O_5$ materials oxidize at lower temperatures, comparing to unmodified $BaYMn_2O_5$. Due to higher molar mass of Gd, comparing to Y, the reversible oxygen storage capacity decreases with the increasing content of gadolinium, but for all measured materials is higher, in comparison to commercial $Ce_{0.5}Zr_{0.5}O_2$. The obtained results are promising, and indicate possibility of further modification of $BaYMn_2O_{5+\delta}$.

Acknowledgements

The project was funded by the National Science Centre Poland (NCN) on the basis of the decision number DEC-2011/01/B/ST8/04046.

Literature

1. Züttel, A., Borgschulte, A., Schlapbach, L. (eds.): Hydrogen as a Future Energy Carrier, WILEY-VCH, 2008.
2. Tsinoglou, D.N., Koltsakis, G.C., Peyton Jones J.C.: Oxygen Storage Modeling in Three-Way Catalytic Converters. Industrial & Engineering Chemistry Research 2002, **41**, 1152
3. Sugiura M.: Oxygen storage materials for automotive catalysts: ceria-zirconia solid solutions. Catalysis Surveys from Asia 2003, **7**, 77
4. Machida, M., Kawamura, K., Kawano, T., Zhang, D., Ikeue, K.: Layered Pr-dodecyl sulfate mesophases as precursors of $Pr_2O_2SO_4$ having a large oxygen-storage capacity. Journal of Materials Chemistry 2006, **16**, 3084
5. Motohashi, T., Ueda, T., Masubuchi, Y., Takiguchi, M., Setoyama, T., Oshima, K., Kikkawa, S.: Remarkable Oxygen Intake/Release of $BaYMn_2O_{5+\delta}$ Applications of Oxygen Storage Technologies. Chemistry of Materials 2010, **22,** 3192
6. King, G., Woodward, M.: Cation ordering in perovskites, Journal of Materials Chemistry 2010, **20**, 5785
7. Larson, A.C., Von Dreele, R.B.: Los Alamos Natl. Lab. Rep. – LAUR 86–748 2004
8. Toby, B.H.: EXPGUI, a graphical user interface for GSAS. Journal of Applied Crystalography 2001, **34**, 210
9. Millange, F., Suard, E., Caignaert, V., Raveau, B.: $YBaMn_2O_5$: Crystal and Magnetic Structure Reinvestigation. Materials Research Bulletin 1999, **34**, 1
10. Nakajima, T., Kegeyama, H., Ueda, Y.: Successive phase transition in a metal-ordered manganite perovskite $YBaMn_2O_6$. Journal of Physics and Chemistry of Solids 2002, **63**, 913
11. Karppinen, M., Okamoto, H., Fjellvåg, H., Motohashi, T., Yamauchi, H,: Oxygen and cation ordered perovskite, $Ba_2Y_2Mn_4O_{11}$. Journal of Solid State Chemistry 2004, **177**, 2122
12. Wiliams, A.J., Attfield, J.P., Ferro-orbital order in the charge- and cation-ordered manganite $YBaMn_2O_6$. Physical Review B 2005, **72**, 024436
13. Klimkowicz, A., Zheng, K., Fiołka, G., Świerczek, K.: Materiały ceramiczne z grupy perowskitów podwójnych na bazie $BaYMn_2O_{5+\delta}$ dla technologii magazynowania tlenu. Materiały Ceramiczne / Ceramic Materials 2013, accepted for publication
14. Gilleßen, M., Lumeij, M., George, J., Stoffel, R., Motohashi, T., Kikkawa, S., Dronskowski, R., Oxygen-Storage Materials $BaYMn_2O_{5+\delta}$ from the Quantum-Chemical Point of View. Chemistry of Materials 2012, **24**, 1910

Grzegorz FIOŁKA – B.Sc., currently he is a second year master student at the Department of Hydrogen Energy, Faculty of Energy and Fuels, AGH.

Alicja KLIMKOWICZ – M.Sc., graduated from the Faculty of Energy and Fuels, AGH University of Science and Technology (2012). Currently she is a first year PhD student in the Department of Hydrogen Energy, Faculty of Energy and Fuels, AGH. Her scientific research covers structure and oxygen storage properties of perovskite-type oxides.

Kun ZHENG – M.Sc., graduated from the Faculty of Materials Science and Ceramics, AGH University of Science and Technology (2011). Currently he is a second year PhD student in the Department of Hydrogen Energy, Faculty of Energy and Fuels, AGH. His research covers crystal structure, electrochemical properties and diffusion processes in mixed ionic-electronic conductors. He is coauthor of 5 articles in scientific journals from Thomson Reuters Master Journal List.

e-mail: zheng@agh.edu.pl

Konrad ŚWIERCZEK – Ph.D., he obtained his PhD degree in materials science at the Faculty of Materials Science and Ceramics, AGH University of Science and Technology in 2002, which was followed by habilitation degree in 2011. Currently he works as AGH professor at the Department of Hydrogen Energy, Faculty of Energy and Fuels, AGH. His research concerns relationship between crystal structure and transport properties of mixed ionic-electronic conductors used in Solid Oxide Fuel Cells and Lithium-ion batteries. He is co-author of 40 articles in scientific journals from Thomson Reuters Master Journal List.

e-mail: xi@agh.edu.pl; phone: +48 12 617 4926